Journal of Pharmaceutical Sciences 113 (2024) 625–636

Contents lists available at ScienceDirect

Journal of Pharmaceutical Sciences

journal homepage: www.jpharmsci.org

Pharmaceutical Biotechnology

Exploring a Role for Flow-Induced Aggregation Assays in Platform Formulation Optimisation for Antibody-Based Proteins

Leon F. Willis[a], Vishal Toprani[b], Sashini Wijetunge[b], Annette Sievers[c], Laura Lin[c], Jeanine Williams[d], Tom J. Crowley[b], Sheena E. Radford[a], Nikil Kapur[e], David J. Brockwell[a,*]

[a] *Astbury Centre for Structural Molecular Biology, School of Molecular and Cellular Biology, Faculty of Biological Sciences, University of Leeds, Leeds LS2 9JT UK*
[b] *Pharmaceutical Research and Development, Pfizer Inc. 1 Burtt Road, Andover, Massachusetts 01810, USA*
[c] *BioMedicine Design, Pfizer Worldwide Research & Development, 610 Main Street, Cambridge, MA 02139, USA*
[d] *School of Chemistry, Faculty of Engineering and Physical Sciences, University of Leeds, Leeds LS2 9JT, UK*
[e] *School of Mechanical Engineering, Faculty of Engineering and Physical Sciences, University of Leeds, Leeds LS2 9JT, UK*

ARTICLE INFO

Article history:
Received 17 July 2023
Revised 23 October 2023
Accepted 23 October 2023
Available online 30 October 2023

Keywords:
Antibody
Aggregation
Developability screening
Protein aggregation
Protein formulation
Physicochemical properties

ABSTRACT

The development time of therapeutic monoclonal antibodies (mAbs) has been shortened by formulation platforms and the assessment of 'protein stability' using 'developability' assays. A range of assays are used to measure stability to a variety of stresses, including forces induced by hydrodynamic flow. We have previously developed a low-volume Extensional Flow Device (EFD) which subjects proteins to defined fluid flow fields in the presence of glass interfaces and used it to identify robust candidate sequences.
Here, we study the aggregation of mAbs and Fc-fusion proteins using the EFD and orbital shaking under different formulations, investigating the relationship between these assays and evaluating their potential in formulation optimisation. EFD experiments identified the least aggregation-prone molecule using a fraction of the material and time involved in traditional screening. We also show that the EFD can differentiate between different formulations and that protective formulations containing polysorbate 80 stabilised poorly developable Fc-fusion proteins against EFD-induced aggregation up to two-fold. Our work highlights common platform formulation additives that affect the extent of aggregation under EFD-stress, as well as identifying factors that modulate the underlying aggregation mechanism. Together, our data could aid the choice of platform formulations early in development for next-generation therapeutics including fusion proteins.

Introduction

Monoclonal antibodies (mAbs) have emerged as effective therapeutics[1,2] due to their high affinity[1] and specificity[2] against an ever-broadening range of disease targets,[3,4] employing mechanisms beyond that of simple receptor (ant)agonism.[3,5] In accord with their need to bind multiple targets (either on different cells[6] or on targets in solution),[7] these next-generation therapeutics, which are mostly based on mAb scaffolds, display a startling array of designs.[8] For example, over 30 Fc-fusion proteins are currently in clinical trials against a range of disease targets.[9,10]

One of the many hurdles facing the successful development of protein-based molecules as drugs is their tendency to aggregate.[11,12] Aggregation is typically instigated by the partial or complete unfolding of protein molecules, followed by their self-association.[13,14] The formation of aggregates can increase processing costs due to the need to remove them,[12] as they can illicit adverse immunogenic and pharmacological effects in patients.[15,16] While one could re-engineer a protein to make it less likely to aggregate,[17,18] a common strategy to improve the physicochemical behaviour of a protein is to change its solution conditions.[11,19] This task has been facilitated by the academic and industrial knowledge accrued over the last 30 years, allowing the development of so-called 'platform manufacture'[20] and formulations.[21,22] By optimising mAb manufacture and formulation

Abbreviations: AS, Accelerated Stability; ANOVA, analysis of variance; BSA, Bovine serum albumin; DLS, Dynamic light scattering; EFD, Extensional Flow Device; Fc-XEng, Fragment crystallisable- protein X engineered variant fusion; Fc-XWT, Fragment crystallisable- protein X wild-type fusion; HS, histidine-sucrose; HSA, histidine-sucrose-arginine; OD_{350}, optical density at 350 nm (turbidity); PS80, polysorbate 80; SE-HPLC, Size-exclusion high-performance liquid chromatography; UV–Vis, Ultraviolet-Visible spectrophotometry.

* Corresponding author.
E-mail address: d.j.brockwell@leeds.ac.uk (D.J. Brockwell).

https://doi.org/10.1016/j.xphs.2023.10.031

via small changes within defined areas of parameter space, platform approaches reduce development time,[23] reducing the height of the barrier to commercialization.[19] The applicability of these platforms to the manufacture of more unusual and complex modalities, including Fc-fusions, is currently unclear, and there is thus an increased focus on the development of rapid and facile methods to optimise biopharmaceutical formulation.[24]

An array of assays is commonly employed to optimise the formulation of a protein of interest.[23,25–28] Accelerated stability (AS) methods are routinely used by industry as part of 'developability' assessments, probing the affinity and specificity of candidates and their behaviour in response to changes in temperature,[29] pH[30] and ionic strength.[31–34]

In addition to these well-defined biophysical perturbants, therapeutic proteins are exposed to agitation, various interfaces (both air: liquid and liquid:solid) and a variety of hydrodynamic flow fields, throughout their lifetime from manufacturing[12,35] and transport[36] through to parenteral delivery into the patient.[37–39] Several developability assays have consequently been designed to mimic mechanically-induced stresses such as shaking during transport.[40] To complement these assays,[41–48] we have recently developed a low-volume Extensional Flow Device (EFD, Fig. 1A), which subjects proteins to an extensional flow field (with a velocity gradient generated in the direction of flow), followed by a shear flow (with a velocity gradient perpendicular to the direction of flow). Unlike shear flow, extensional flow fields, have been shown to induce conformational changes for proteins evolved to be flow responsive and are found throughout manufacturing, including during filtration.[35] The ability of hydrodynamic flow alone (i.e. in the absence of any interfaces) to induce conformational changes for globular proteins remains controversial (see Discussion).[49] Irrespective of the precise mechanism of action, we have showed that the EFD can identify aggregation-prone mAbs, suggesting a role in developability pipelines.[49,50] By assessing the relationship between the results of EFD experiments and biophysical developability assays, we showed that the EFD sits on a unique branch on a 'family tree' of developability assays used to characterise clinically relevant sequences.[51,52] The relationship between the EFD and potentially related assays such as mechanical shaking assays, remained unexplored.

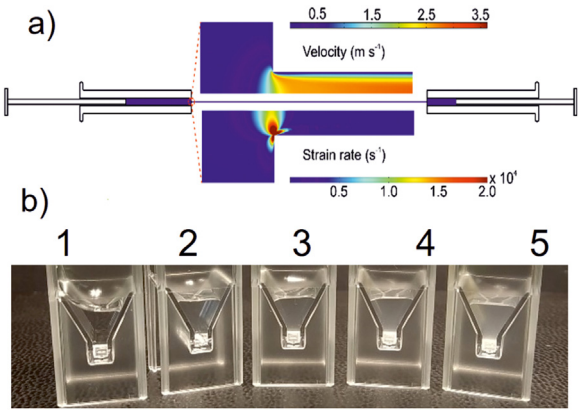

Figure 1. Using an Extensional Flow Device (EFD) to trigger protein aggregation. a) The EFD comprises two Hamilton syringes connected by a borosilicate glass capillary. Shuttling 0.5 mL of protein solution between the syringes results in an extensional flow at the contraction point between syringe and capillary. Computational Fluid Dynamics (CFD) analysis shows the increase in fluid velocity (top), as well as the strain rate (bottom), which quantifies the extensional flow. A harsh shear flow (shear rate ~50,000/s) is present along the capillary. Image taken from Willis et al. 2018 using a CC-BY 4.0 license.[50] b) Representative image (n = 3 biological repeats) of 0.5 mg/mL mAbP2 solution after: 1) 0, 2) 50, 3) 100, 4) 150 and 5) 200 passes in the EFD. The sample was in HS buffer (20 mM L-His and 8.5 % (w/v) sucrose, pH 5.8).

In addition to a role in candidate selection, we also previously showed that a buffer containing arginine and succinate reduced the EFD-induced aggregation of an IgG1.[50] Despite this success, the ability of the EFD (which uses milligram quantities of protein over a timescale of minutes) to assess the effectiveness of a range of commonly employed platform biopharmaceutical formulations (that comprise common additives across different modalities)[22] remained unexplored.[19,23]

Herein, the aggregation behaviour of a panel of eight IgG1 and IgG2 molecules (mAbP1–8), selected for their diverse behaviour under thermal stress, was assessed by conventional shaking stress, as well as with the EFD in a histidine-sucrose (HS) platform buffer. General patterns of aggregation propensity under flow are shared by the antibody panel, with differences observed between the data generated with EFD and orbital shaking, suggesting these methods induce protein aggregation through different mechanisms. For a subset of the panel (mAbP3–6), by systematically varying: protein concentration, platform buffering agent, pH, co-solutes and surfactants, we show that the EFD can differentiate protein behaviour between the formulations. The knowledge gained from the mAbP3–6 panel was then applied to two Fc-fusion proteins, with polysorbate 80 (PS80) emerging as a protective excipient against EFD-induced stresses, as aggregation of the fusion proteins was reduced by up to two-fold. Comparison of the rank of aggregation propensity for each protein under EFD and orbital shaking stress and the effects of buffer composition on these ranks, reveals that these assays probe different biophysical liabilities. By reporting on flow-induced aggregation (which may be a convolution of hydrodynamic and surface-induced effects) the EFD complements other developability assays and may be especially useful in rapidly identifying stabilising formulations early in development, especially for off-platform next-generation therapeutics. It may also be used to preferentially select molecules which fit the platform formulation.

Materials and Methods

Formulation Buffers

Histidine-sucrose (HS): 20 mM L-histidine hydrochloride (Sigma Aldrich) and 8.5 % (w/v) sucrose (Fisher), pH 5.8 was prepared in Leeds, dissolving the components in 18 MΩ H_2O and titrating with HCl (Fluka). The buffer was filtered through a 0.22 μm Durapore membrane (Merck Millipore) and stored at 4 °C for no longer than a week.

Tris-sucrose (TS): 20 mM Tris hydrochloride (Sigma Aldrich and Biospectra) and 8.5 % (w/v) sucrose (Pfantstiel), pH 7.5 was prepared by Pfizer, frozen and shipped to Leeds together with the corresponding protein samples on dry ice. The buffer was thawed, used and stored in the same fashion as the HS buffer.

Histidine-sucrose-arginine (HSA): 20 mM L-histidine (Sigma Aldrich), 8.5 % (w/v) sucrose (Pfantstiel) and 20 mM L-arginine hydrochloride (Ajinomoto), pH 5.8 was prepared by Pfizer, frozen and shipped as above.

Polysorbate 80 (PS80): a stock of 10 % (w/v) PS80 (JT Baker) was prepared in 18 MΩ H_2O, filtered (0.22-μm, Merck Millipore) and kept in the dark at 4 °C. When required, PS80 was added to a final concentration of 0.02 % (w/v)), assuming a stock density of 1 g/mL. Protein concentration adjustment was then performed as stated below.

Protein Sample Preparation

The EFD 1–8 mAbs and the Fc-WT and Fc-XEng fusion proteins were produced from stable Chinese Hamster Ovary cell expression. Further details on the isotypes of mAbP1–8 are in Table S2. The

proteins were transported on dry ice and stored at - 80 °C until required. For flow experiments (mAbP1–8) frozen stock solutions (20 mg/mL) were thawed at room temperature and diluted ~1:5 with His-sucrose buffer. After filtration (0.22-μm filter, Millipore), the sample was subsequently diluted 10-fold to determine the concentration by UV–Vis spectroscopy, at 280 nm using an extinction coefficients in Table S2 and diluted to 0.5 or 5 mg/mL as required and kept on ice. mAbP3–6 in TS and HSA buffers were supplied by Pfizer and treated in a similar fashion as above, except a final concentration of 5 mg/mL was used.

To make 27.5 mg/mL and 50 mg/mL protein solutions (mAbP3 and 5), 1 mL thawed stock solution (50 mg/mL) was clarified using a bench-top centrifuge at 13,000 *xg* for 10 mins. 900 μL of supernatant was removed and then either diluted to 27.5 mg/mL or used directly. All sample solutions were kept on ice.

Fc-fusion proteins were thawed and clarified by syringe filtration, assuming the shipment concentrations of 7.4 mg/mL for WT and 6.7 mg/mL Fc-XEng). For the formulation screen, protein samples in HSA were prepared by buffer exchange (Zeba desalting columns, ThermoFisher), according to the manufacturer's protocol. When required, PS80 was added to the samples after buffer exchange to a final concentration of 0.02 % (w/v). The protein was then kept on ice, as stated above.

The panel of proteins in different buffers were aliquoted, snap frozen in liquid nitrogen and stored at −80 °C until further use. No more than one subsequent freeze-thaw cycle was performed with each sample.

Hydrodynamic Stress Experiments Using the Extensional Flow Device (EFD)

Full details regarding the EFD can be found elsewhere.[49] Briefly, in EFD experiments, a sample volume of 0.5 mL of protein solution was drawn into a Gastight 1001RN Hamilton Syringe though a 0.3 mm (i.d.) Sutter instruments glass capillary, with air-bubbles removed. Following connection to a second syringe *via* ferrule compression connectors (Hamilton) and a Gilson P10 O-ring (Gilson), the samples were stressed for up to 200 passes. The plunger velocity was either 4-, 8- or 16 mm/s, with plungers driven by a stepper motor, controlled through an Arduino microprocessor. The length of time per pass, strain rate and shear rate at these plunger velocities, are summarised in Table S3. Quiescent samples for each experiment were prepared by incubating the same protein solution at ambient temperature for the same time as the longest experiment, e.g. 200 passes at 4 mm/s takes 40 min.

Following stress, the sample was slowly decanted into a fresh Eppendorf and kept on ice until analysis (see below). The capillary was discarded, the syringes cleaned with 2 % (v/v) Hellmannex-III solution (Hellma Analytics), 18 MΩ water, then 0.5 mL of the appropriate platform formulation buffer, prior to processing the next sample.

Visual Inspection

Prior to analysis by turbidity and HPLC monomer loss, 250 μL of the protein sample was transferred into a clean Starstedt polystyrene UV–Vis cuvette. The cuvettes were photographed against a black background, illuminated by a lamp ~30 cm above. Images were taken with an 8-megapixel mobile phone camera and cropped to size in Microsoft PowerPoint 2016.

Turbidity Measurements

The optical density of samples at 350 nm was recorded using Shimadzu 1800 UV–Visible spectrophotometer, after blanking against the respective platform formulation buffer.

HPLC Monomer-Loss Assays

3 × 150 μL of each quiescent or stressed sample was clarified by ultracentrifugation at 4 °C for 30 min at 35,000 *xg* (TLA100 rotor in an Optima TLX centrifuge, Beckmann Coulter) and 300 μL supernatant of each sample transferred to a 300 μL conical insert polypropylene HPLC vial (VWR). After being crimp-sealed with aluminium/PTFE lids (ThermoFisher), vials were stored on ice until HPLC analysis.

The work in this manuscript was performed during the COVID-19 pandemic, precluding the use of one HPLC system for the duration of the project in Leeds, UK. For transparency to the reader, HPLC analysis was performed for ~thirty 0.5 mg/mL mAbP1–8 samples on a Dionex HPLC system, before moving to Agilent 1400 (School of Chemistry, University of Leeds) system for the 0.5 and 5 mg/mL HS studies, in addition to the initial round of Fc-fusion protein experiments (Fig. S9). The 27.5 and 50 mg/mL HS studies, HS + PS80, TS, HSA (+/- PS80) and final Fc-Fusion screens were analysed with a biocompatible Shimadzu Nexera HPLC system. The injection volume used was 20 μL on the latter two systems, where the majority (> 95 %) of all data were collected. Two technical replicates were run for each quiescent sample, with the average loading error across all replicates used to assess the noise in the experiment, in addition to capturing differences between the systems.

On all systems, samples were applied to a YMC Pack Diol 200 gel-filtration column, operated at 0.75 mL/min with 20 mM sodium phosphate + 400 mM NaCl, pH 7.2, as the mobile phase. All samples were kept at 4 °C in the autosampler. The run length was 23 min for Agilent instruments or 21 min on the Shimadzu system. Elution was tracked at 280 nm using a photodiode array detector on all systems. Peak areas were integrated using Chromeleon (Dionex and Agilent systems) or LabSolutions (Shimadzu) software.

Data Processing and Analysis

The number of replicates is specified in each figure legend. Numerical data were processed in Microsoft Excel, including ranking of data for Spearman's rank analysis using the RANK.AVG function. One-way ANOVA calculations and Spearman's rank correlation analyses were performed in Origin Pro 2022. All graphs were also plotted with this software.

Supplementary Methods

Details of Dynamic Light Scattering (DLS) measurements, real-time (5 °C) and accelerated (25 °C) stability and orbital shaking are provided in the Supplementary Methods.

Results

A Histidine-Sucrose (HS) Platform Formulation Leads to Common Behaviours in the Extent and Growth of mAb Aggregates Under Flow

As the basis for this study, eight mAbs from the Pfizer inventory were selected. Accelerated (AS) (25 °C) and real-time (5 °C) stability data are available for seven of these (mAbP1–7, Fig. S1), with mAb aggregation monitored using Size Exclusion, High-Performance Liquid Chromatography (SE-HPLC). (Note: As these data were accumulated prior to the initiation of the study reported here, the formulations were similar, but not identical, generally comprising: L-histidine buffer with carbohydrate co-solutes, surfactant and, in some cases, chelating agent and anti-oxidant, pH 5–6 (Table S1)). The molecule panel, dubbed mAbP1–8 herein, comprises four IgG1s and four IgG2s. To examine whether the EFD induces aggregation in these molecules under the same conditions, all eight EFD mAbs were

formulated in a common histidine-sucrose (HS) buffer, pH 5.8 and stressed under similar flow conditions (Materials and Methods).

As both the number of passes and the plunger velocity are known to affect EFD-induced aggregation,[50] all eight molecules were stressed across the range of 0 to 200 passes at three different plunger velocities (4-, 8- and 16 mm/s), comprising low, medium and high hydrodynamic stress conditions, respectively. Analysis of the samples by visual inspection showed that all the samples became turbid as a function of pass number (Fig. 1b and Fig. S2), with this being most pronounced following stress at the highest velocity (16 mm/s) and highest pass number (200). Notably, none of the quiescent samples were visibly turbid. While there were no clear, or consistent, changes in sample turbidity as a function of plunger velocity across the mAb panel, on close visual inspection, the particles appeared larger (to the eye) in the 4 mm/s series versus their counterparts at higher plunger velocities.

To quantify the extent of turbidity in the samples, the optical density of the sample at 350 nm was measured (OD_{350}, Methods). The data in Fig. 2 show that the increase in sample turbidity correlates with pass number at all three plunger velocities, in agreement with the observations made above. The turbidity measurements showed that gradient of the turbidity:pass number line increased with plunger velocity (Fig. 2a-c).[46] To understand whether the plunger velocity affected the size of EFD-induced aggregates, Dynamic Light Scattering (DLS) measurements were performed on mAbP4, chosen as an example of a highly aggregating sample. After being stressed for 50 passes, an increase in sample dispersity was observed at 8 and 16 mm/s suggesting the formation of larger aggregates under these conditions (Fig. 2d).

All of the mAbs studied showed an increase in pass number dependence on OD_{350} as a function of plunger velocity, but with no significant differences in gradient between the panel members (Fig. S3). As the complex relationship between scattering intensity, particle size and number renders the data from these semi-quantitative methods[53] challenging to interpret in terms of quantitating absolute aggregation levels, aggregation was also measured by quantifying the loss of monomer by SE-HPLC, following clarification by ultracentrifugation (Methods). As SE-HPLC quantifies only the monomer remaining in solution (via its ability to enter the resin matrix), it is insensitive to the type of higher-order species formed. As both pass number and plunger velocity affect the extent of EFD-induced aggregation,[50] a three-dimensional aggregation landscape (Fig. 3) is required to visualise a protein's liability to EFD-induced aggregation. The landscapes of the mAbP1–8 panel (Fig. 3 and Fig. S4) are broadly similar with a simple planar topology, showing that for these IgGs, aggregation changes only marginally with plunger velocity (in contrast to a previously studied IgG1, STT[50] (Fig. 3c). Despite the similarity of the surface topology, the gradients differed, with mAbP1 and

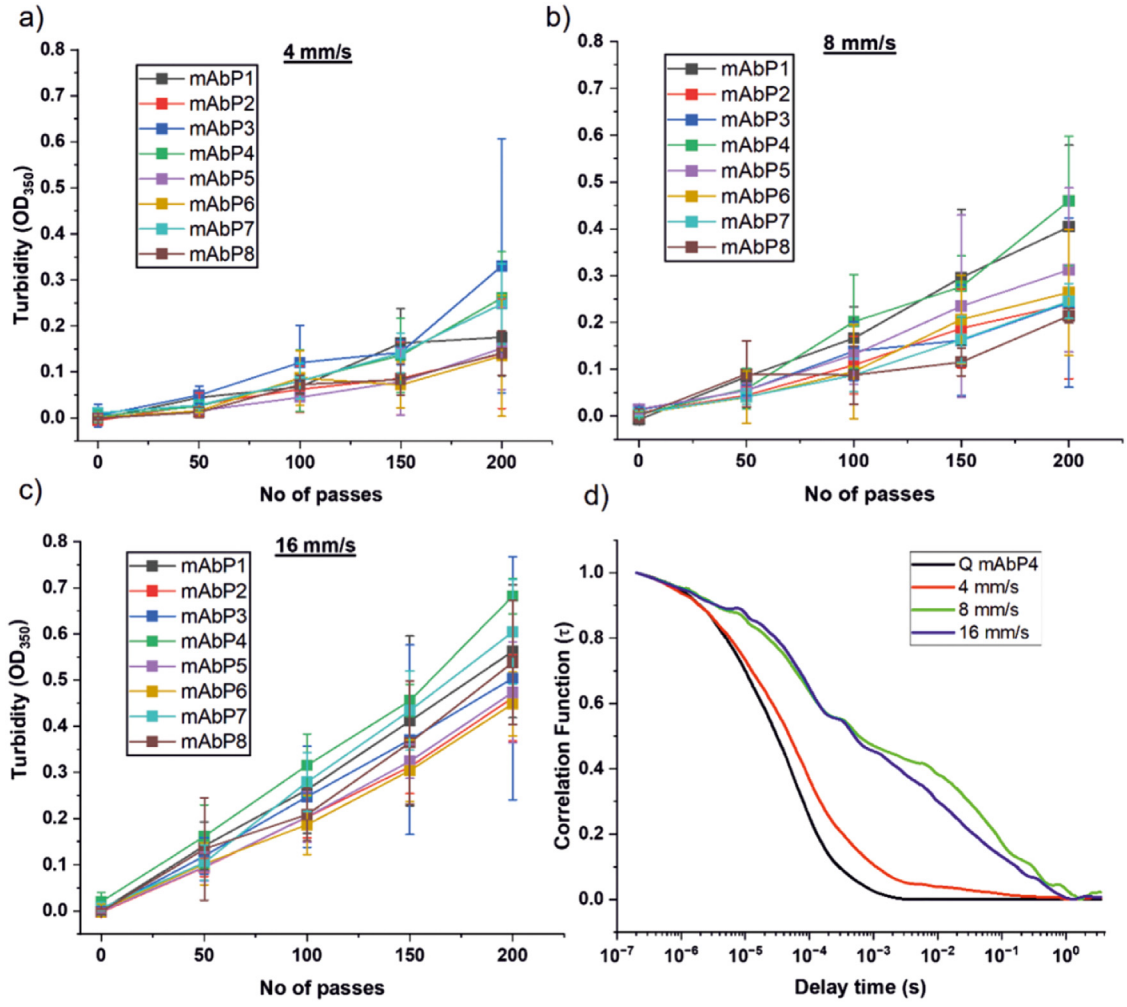

Figure 2. Quantification of EFD-induced antibody aggregation using light scattering. Turbidity (OD_{350}) of 0.5 mg/mL mAbP1–8 samples in HS buffer after 0, 50, 100, 150 and 200 passes in the EFD at a plunger velocity of a) 4 mm/s, b) 8 mm/s and c) 16 mm/s. n = 3 biological repeats, error bars = s.d. d) Correlation function for 0.5 mg/mL mAbP4, either quiescent (Q) or following 50 passes in the EFD at 4-, 8- or 16 mm/s, examined using Dynamic Light Scattering (DLS). n = 2 biological repeats, with representative traces shown. Sample dispersity was notably higher in the 8- and 16 mm/s samples. Nanoparticles present in the sucrose formulation,[87] confirmed experimentally by DLS of buffer in the absence of protein and sucrose, account for the deviation from a smooth single-exponential decay describing the correlation function of a monomeric mAb by DLS, as seen previously.[49]

mAbP5 and 8 showing the least and greatest dependence, of monomer loss on pass number, respectively (Fig. 3a,b). Accordingly, the sensitivity of mAbP1–8 to EFD-induced aggregation were ranked by calculating the average % monomer loss across the three plunger velocities, then fitting a straight line to the data to determine the apparent rate (Fig. 3d). These data show that under these initial conditions, the average apparent rate of monomer loss ranged from ~0.26–0.37 % monomer loss per pass, with mAbP1 at the bottom of this range. While the differences in rates are, again, similar to one another, mAbP5 and 8 were found to be significantly more aggregation prone than the most stable molecule, mAbP1. Currently, as with other development assays,[23,54] the ability of the EFD to predict the long-term and accelerated stability of mAbs is unknown. Here, despite difference in buffers between EFD-induced aggregation experiments and the AS dataset (which themselves are in different formulations, that precludes formal analysis), it can be seen, that at 25 °C (where relatively large differences are observed in thermal stability) mAbP1 is the most stable molecule. The trends in the AS data and those obtained from the EFD using ~4 mg protein and an experimental time of ~6 h, including clarification, per replicate) suggests that the EFD dataset accumulated in these preliminary experiments, may be able to identify extremely good or bad candidates for development with poor differentiation for moderately stable candidates. Further experiments comparing the relative stability (in terms of monomer loss over time) of a panel of mAbs, in the same buffer subjected to EFD stress and incubated over time at 5 °C and 25 °C, would be required to confirm this observation, as would the identification of EFD conditions which enhance the dynamic range of the data.

Orbital shaking assays (where glass vials containing protein solution are continuously agitated) are commonly used during development to assess the stability of mAbs to interfacial stresses.[33,36,55] To explore the relationship (if any) between this assay and the EFD, 0.5 mL of each mAb was shaken in an orbital shaker at 0.5 mg/mL in HS buffer, at 300 rpm for between 4 and 24 h (Methods). After 4 hrs, the extent of monomer loss observed ranged from 0.9 to 9.7 %, with four mAbs (mAbsP4,5, 6 and 7) showing the least aggregation. After 24 h much larger differences between the molecules are observed, Fig. S5. The panel could be arbitrarily grouped into molecules

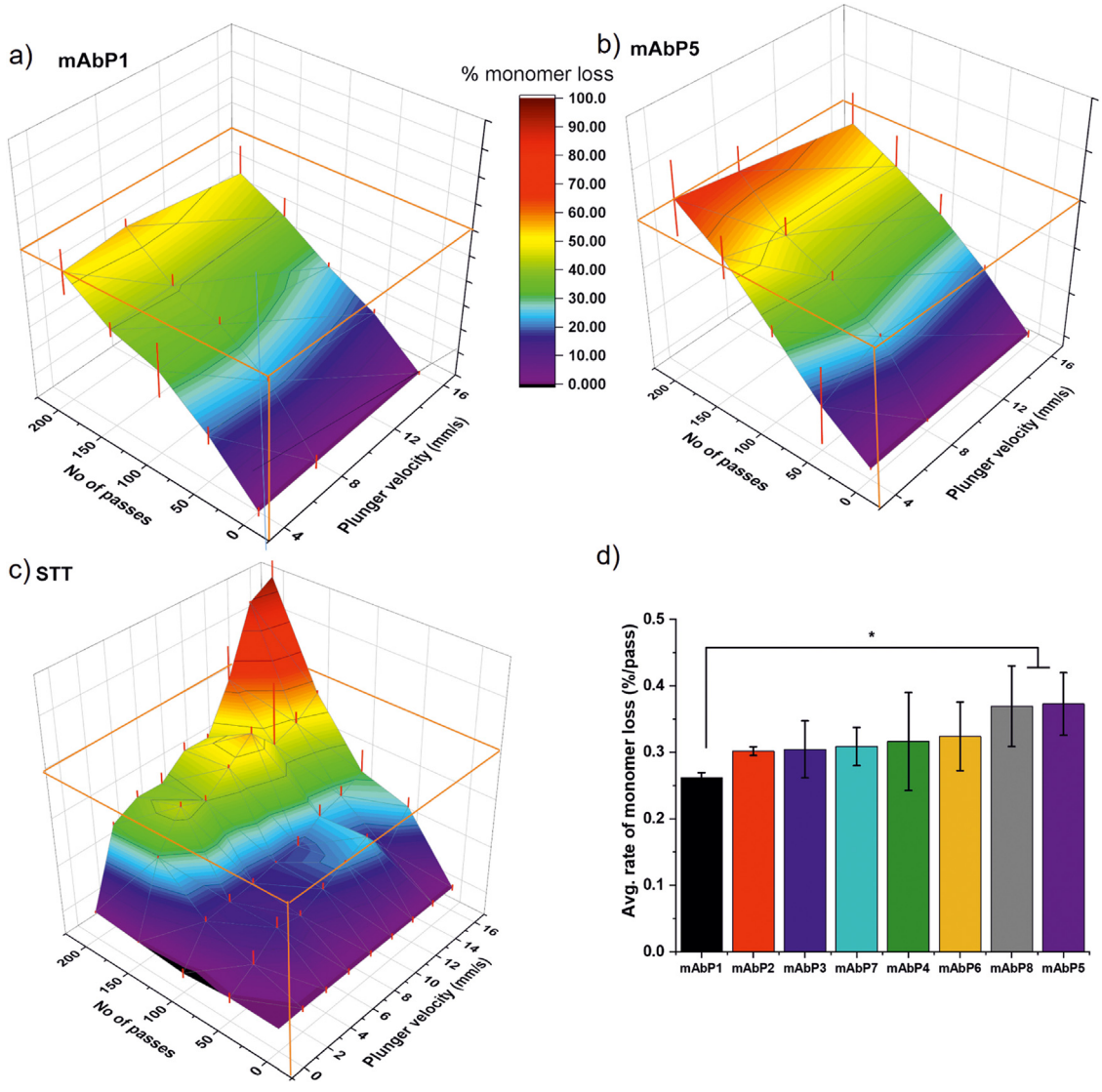

Figure 3. Percentage monomer-loss antibody aggregation landscapes. Landscape analyses for a) mAbP1 and b) mAbP5. EFD-induced aggregation as a function of pass number and plunger velocity was quantified using HPLC (Methods). mAbs were at 0.5 mg/mL in HS buffer. n = 3 biological repeats, error bars (in red) = s.d. Fifteen pass number and velocity values (in triplicate) comprise each landscape. c) Plot of STT IgG1 data from Willis et al. 2018,[50] showing speed-dependent aggregation of this antibody at 0.5 mg/mL. n = 2, error bars = s.d. The orange frames in a–c are to guide the eye, set at 60 % aggregation. d) Average rate of monomer loss (%/pass) for the mAbP1–8 molecules, as determined from a linear fit to the % monomer loss under each pass condition. Rate = gradient, error bar = fit error. * = p-value ≤0.05.

showing the highest levels of monomer loss (greater than 10 %, mAbP3 and 5), intermediate levels (between 5 and 10%, mAbP2, 4,7,8) and those showing resilience to orbital shaking (less than 5 % monomer loss, mAbP1 and 6). Spearman's rank correlation was performed to compare the rates of monomer loss observed from the EFD with the extent of monomer loss from orbital shaking. A negative correlation was observed between the EFD and orbital shaking data after 4 hrs (Spearman's correlation coefficient = −0.64) with a weaker correlation seen between the EFD and 24 hr orbital shaking data (Spearman's correlation coefficient = 0.12). Together, the differences observed between these methods (Table S4) suggest that the underlying mechanisms of protein aggregation induced by orbital shaking and the EFD may be different (see Discussion),[46] with the timescale of the former method playing an important role in the extent of aggregation observed.[48]

Protein Concentration Impacts the Extent of mAb Aggregation Under Flow

As the degree of aggregation is quantified using SE-HPLC in the EFD assay, the experiment typically uses dilute protein solutions (0.5 mL at a concentration of 0.5 mg/mL). While advantageous in terms of sample requirements, such low concentrations are rarely found during downstream processing and formulation in mAb manufacture. To reflect these conditions, accelerated stability studies are typically carried out at final drug product concentrations[56] (>10 mg/mL[22]) that are 20–100 fold higher than used in the EFD. In order to determine how protein concentration impacts the trends observed with respect to EFD-induced aggregation, a subset of molecules from the initial panel (mAbP3–6) were stressed for 50 and 200 passes at a plunger velocity of 8 mm/s, at concentrations of 5 and 50 mg/mL in HS buffer.

Visually, the macroscopic extent of aggregation of 5 and 50 mg/mL solutions after 200 passes at 8 mm/s (Fig. S6a) were much greater than the experiments performed at 0.5 mg/mL (Fig. 1), as expected. Using DLS (Methods), protein aggregates were detectable in mAbP4 samples even after 50 passes at 8 mm/s at 5 mg/mL (Fig. S6b), as we previously observed for BSA when stressed in the EFD at the same protein concentration.[50]

To investigate the effects of protein concentration on EFD-induced aggregation in more detail, the extent of EFD-induced aggregation (loss of monomer) was quantified by SE-HPLC for mAbP3–6 at 5 and 50 mg/mL and compared to the data obtained above at 0.5 mg/mL (extracted from Fig. 3). The extent of aggregation was calculated in absolute terms (amount of monomer lost, Fig. S7) and relative terms (percentage monomer loss relative to a control not exposed to EFD stress, Fig. 4). These results show, firstly, that when using data from a single pass number, greater differentiation is apparently achieved at an intermediate concentration, suggesting once again that mAbP5 is the most aggregation prone. However, as these data are derived from fewer biological repeats relative to the data in Fig. 3, this difference was not statistically significant. The advantages of greater differentiation are balanced by the increasing error at higher concentrations, resulting in the adoption of experimental EFD parameters of 5 mg/mL, 200 passes in further experiments. Secondly, while the absolute amount of aggregation increases with protein concentration, the relative amount of aggregate (expressed as percentage of monomer lost) decreases with increasing initial protein concentration (Fig. S7). This inverse concentration-dependence of EFD-induced aggregation, suggests that the underlying aggregation mechanism may change when one moves from low protein concentrations (mediated by surface interactions),[13,57] to high concentrations (at which flux through a bulk mediated pathway increases due to saturation of the surface-mediated pathway). Plotting the relative monomer loss against the initial protein concentration (Fig. S7) shows that such a switch occurs between 0.5 and 5 mg/mL. These data suggest that the solid-liquid interfaces of the EFD play a major role in the aggregation observed following stress in the device, as suggested by others recently.[31,44]

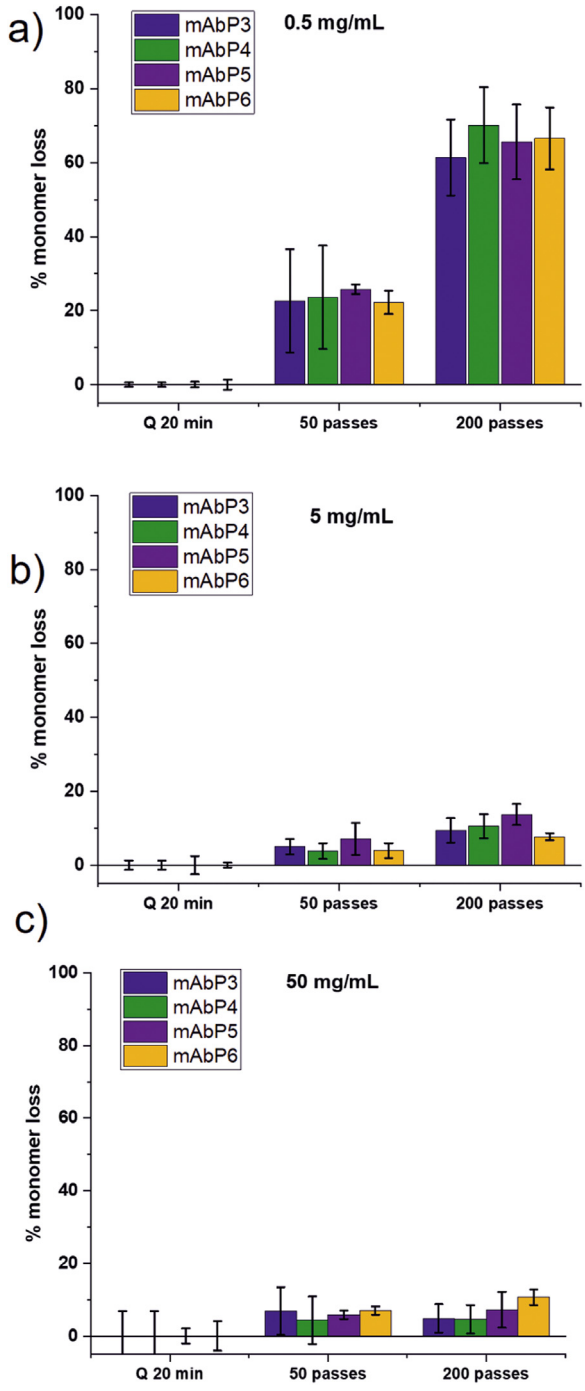

Figure 4. Inverse concentration-dependence of EFD-induced aggregation for mAbP3–6 in HS buffer. a)% monomer loss for 0.5 mg/mL antibody, stressed at 8 mm/s for 0 (quiescent, Q), 50 or 200 passes. The data are reproduced from Fig. 3 (mAbP5) and S4 (mAbP3, 4 and 6). b)% monomer loss data obtained under the same conditions as a, except with 5 mg/mL antibody. *n* = 3 biological repeats, error bars = s.d. c) % monomer loss data obtained under the same conditions as b, except with 50 mg/mL antibody.

Changing the Platform Formulation Reveals Favourable and Unfavourable Conditions for the mAbP3–6 mAbs Under Flow

In order to investigate how platform formulations modulate the aggregation behaviour of the panel of molecules under flow, the

mAbP3–6 mAbs were stressed at 5 mg/mL under an array of solution conditions. Surfactants are ubiquitous in biopharmaceutical formulations, enhancing the long-term stability of many mAbs by competing with proteins for air-water or solid-water interfaces, thus preventing adsorption-mediated unfolding.[32,48] To determine whether surfactants were also protective to mAbP3–6 under flow, the HS buffer and protein stocks were supplemented with PS80 to a final concentration of 0.02 % (w/v) and EFD experiments were performed at 8 mm/s for 50 and 200 passes. The samples were quantified using the monomer-loss assay, with the data revealing, surprisingly, that only mAbP6 is significantly protected against aggregation by PS80, with a 2-fold decrease in aggregation after 200 passes relative to the HS buffer (Fig. 5 and Fig. S8a).

Next, we sought to investigate how a shift in pH influences EFD-induced aggregation. The formulation was thus changed from HS buffer (20 mM L-His, 8.5 % (w/v) sucrose pH 5.8) to TS buffer (20 mM Tris + 8.5% (w/v) sucrose, pH 7.5) and EFD experiments carried out on mAbP3–6 under the conditions previously found to be most discriminating (8 mm/s, 200 passes, 5 mg/mL). The samples were subsequently analysed using the monomer-loss assay (Fig. S8b) showing that mAbP3 and mAbP4 were significantly more aggregation prone in this buffer. The molecular mechanism underlying this decrease in stability is presently unknown, but for mAb4 (*pI* 7.2) a decrease in colloidal stability may drive aggregation at this pH. Whether this affects the colloidal stability of native or near native states[58] in the bulk pathway or surface:protein interactions in a surface pathway remains to be resolved.

As a final modification, the mAbP3–6 molecules were stressed in HS buffer containing 25 mM L-arginine, pH 5.8 (HSA), in addition to the presence or absence of 0.02 % (w/v) PS80. After performing the monomer-loss assay, the analysis showed surprisingly, that HSA buffer does not protect any of the mAbP3–6 molecules from aggregation relative to HS buffer (Figs. 5 and S8 c,d). Indeed, for mAbP6 (and potentially mAbP4), inclusion of arginine results in an increase in EFD-induced aggregation (from 10.6 ± 2.2 to 15.5 ± 4 % monomer loss after 200 passes for mAbP6). For both mAbP5 and 6, addition of PS80 to the HSA buffer protected against aggregation by 25–50 % (Figs. 5c and d). Notably, mAbP3 and mAbP4 were not protected. It is known that, for example, arginine is not a "universal protector" against protein aggregation as it can destabilize the native state of proteins.[59,60] It is also interesting to note that PS80 and arginine may exhibit partial antagonistic effects as mAbP6 shows a small increase in aggregation (1.6 ± 0.6 %) in the presence of PS80 in HSA relative to HS buffers. This result is also seen to a greater extent with more challenging proteins studied below.

These data show that the EFD can rapidly assess the effect of commonly used formulation excipients on aggregation using small quantities of proteins. Using conditions that allow significant differences

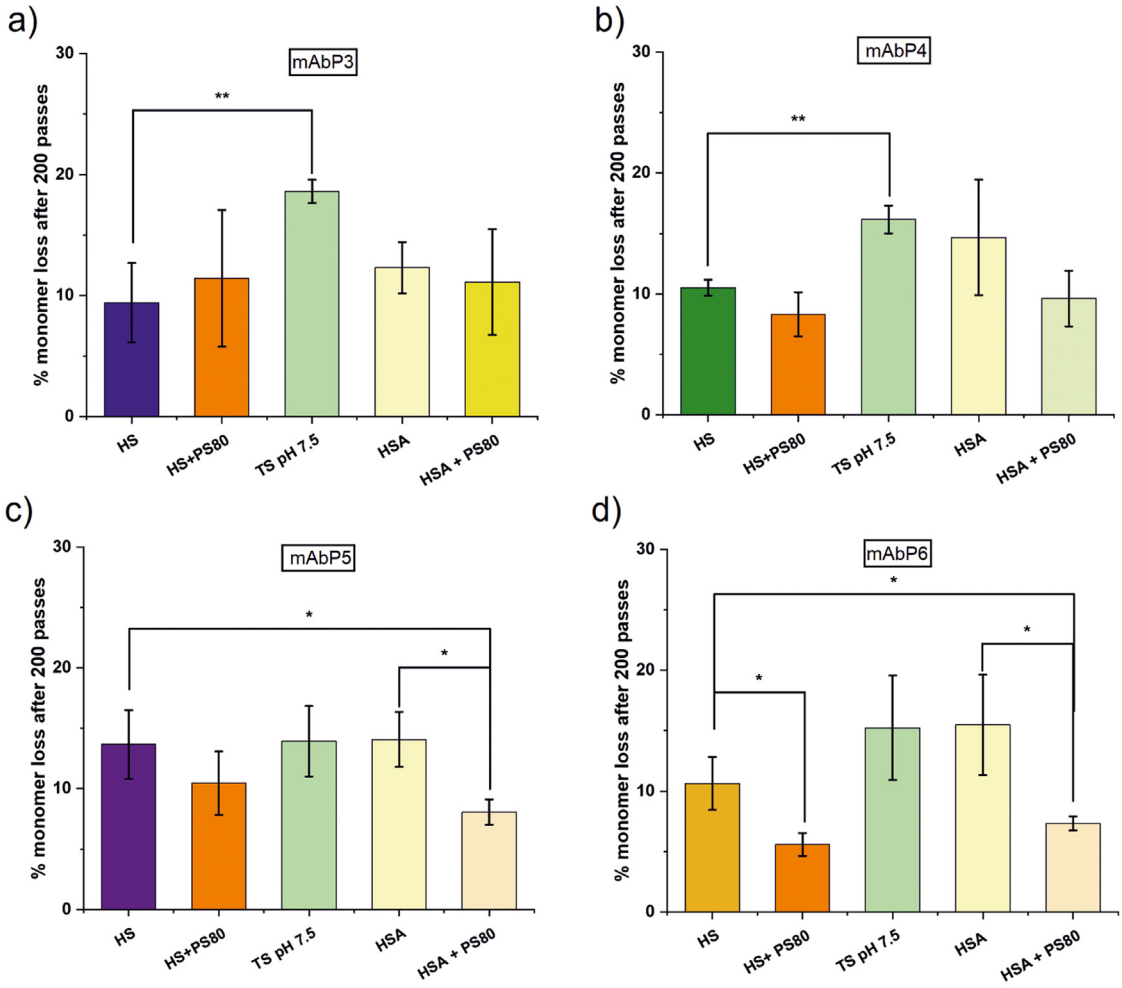

Figure 5. Platform formulation composition modulates the extent of EFD-induced aggregation for a) mAbP3, b) mAbP4, c) mAbP5 and d) mAbP6. All proteins (5 mg/mL) were subjected to 200 passes at 8 mm/s. Data for proteins in histidine-sucrose (HS) buffer are reproduced from Fig. 4. HSA = histidine-sucrose-arginine buffer (Methods). pH = 5.8 for all formulations except Tris-sucrose (TS) = 7.5. PS80 = 0.02 % (w/v) polysorbate 80 present in the samples (Methods). For all data, n = 3 biological repeats, error bars are the standard deviation. Significance was determined using one-way ANOVA: * = p-value ≤ 0.05 and ** = p-value ≤ 0.01.

to be identified, it is clear that the presence of surfactant and the optimisation of pH are the most effective methods of reducing EFD-induced aggregation. In light of the ineffectiveness of arginine under these conditions, it is interesting to note that none of the optimised formulations used for the real-time or AS studies contained this additive (Table S1).

Sensitive Fc-Fusion Proteins can be Protected Against Flow-Induced Aggregation by Protective Platform Formulation Additives

In our previous studies, we mainly investigated the flow-induced aggregation of IgG1 antibodies,[49,51] or globular proteins of varying topology.[50] As there is an increasing number of fusion proteins currently in development,[9,10] which are inherently more sensitive to aggregation that their full-length mAb counterparts,[61,62] we sought to investigate if these scaffolds also exhibited increased sensitivity to EFD-induced aggregation, as well as whether PS80 and/or arginine conferred protection to a pair of Fc- human protein "X" fusion proteins. The pair comprise a wild-type (Fc-XWT) and an engineered variant (Fc-XEng) with improved thermal aggregation propensity (reduced aggregation by SE-HPLC after 4 weeks at 25 °C, data not shown).

Both proteins were initially stressed using the EFD for 0–200 passes under the mAbP1–8 conditions used at the start of the study (0.5 mg/mL, HS buffer, 8 mm/s plunger velocity), given the lower quantity of material available. The HPLC available at the inception of these experiments, which had a stainless-steel flow path, precluded the use of the monomer-loss assay (due to adsorption of the fusion proteins to the flow path, data not shown). Consequently, the extent of soluble protein loss was quantified using an alternative method previously developed in the laboratory,[49] involving clarification by ultracentrifugation followed by spectrophotometric quantification of protein concentration (Fig. S9). The data showed that both molecules are extremely sensitive to flow, with almost 100 % loss of soluble protein after 200 passes (Fig. S9a, note the aggregation levels for mAbP1–8 in the same buffer under in an identical EFD experiment was ~45–70 %).

These experiments were then repeated using the stabilising platform formulation additive identified above (PS80) in both HS and HSA buffers (the latter buffer was included to further investigate potential deleterious competition with PS80 as noted for mAbP4 and mAbP6 above). After stressing Fc-XWT and Fc-XEng at 0.5 mg/mL for 200 passes in these buffers in the presence and absence of surfactant, the monomer-loss assay was performed using a bio-compatible HPLC system (Methods). Firstly, the fusion proteins are far more sensitive to the effects of EFD-stress than standard mAb scaffolds (Figs. 5 and 6), with 94 and 89 % loss of monomer after 200 passes in HS buffer for Fc-XWT and Fc-XEng, respectively. These highlight potential difficulties in their manufacturing in this formulation. This increased sensitivity to EFD-stress results in a large range of responses that in turn reveal large and significant differences between each variant and especially between formulations for the same variant. Notably, Fc-XEng shows less monomer loss than Fc-XWT when stressed in HSA buffer (Fig. S10), which together with the HS result suggests the reduced thermal aggregation propensity of this variant also confers resistance to aggregation by hydrodynamic forces. For both proteins, PS80 reduces EFD-induced aggregation, but this protective ability is reduced in the presence of arginine (~ 2-fold vs 1.25-fold for either protein in HS and HSA buffer, respectively). For these fusion proteins, arginine destabilizes the proteins both directly (with a 5 % (statistically significant), increase in Fc-XWT monomer loss observed when performed in HSA instead of HS) and by reducing the protective effect of surfactant (compare orange and yellow bars in Fig. 6).

Finally, these results were compared to those obtained for Fc-XWT and Fc-XEng after orbital shaking for up to 24 h at 0.5 mg/mL in

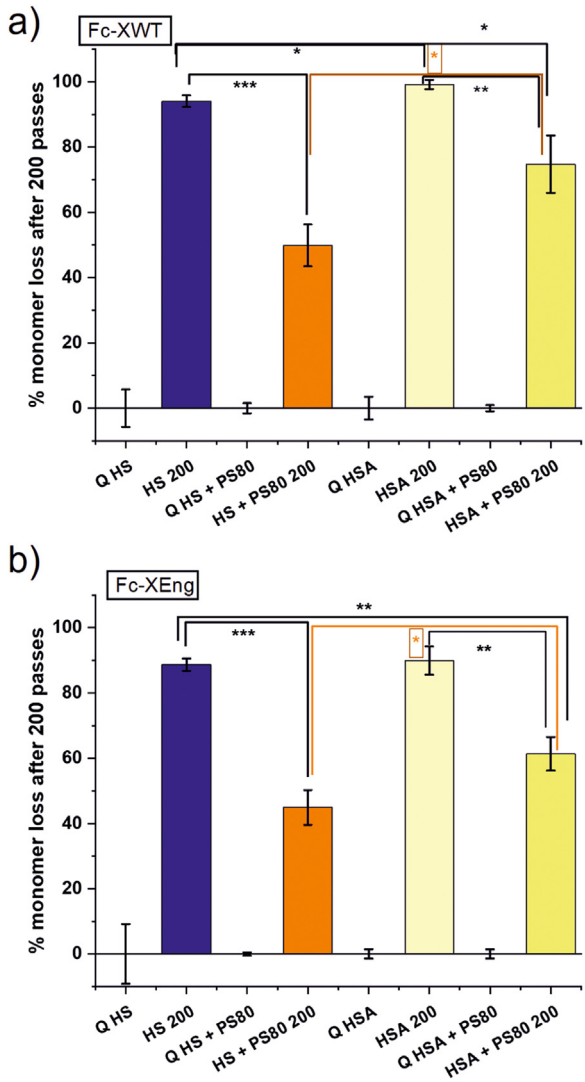

Figure 6. Using the EFD to screen for Fc-fusion aggregation reveals stabilising platform formulations. Plot of percentage of monomer lost after 200 passes in the EFD at 8 mm/s, together with quiescent controls, for a) Fc-XWT and b) Fc-XEng (both at 0.5 mg/mL). HS = Histidine-sucrose, HSA = Histidine-sucrose-arginine, PS80 = 0.02 % (w/v) polysorbate 80. n = 3 biological repeats, error bars show the standard deviation. Significance was determined using one-way ANOVA: * = p-value ≤ 0.05, ** = p-value ≤ 0.01 and *** = p-value ≤ 0.001. Orange brackets are to highlight the differences between the HS and HSA formulations containing PS80.

the same four platform formulations as used in the EFD study (Fig. 7). As shown previously for the mAb constructs, under conditions that allow differentiation between conditions (24 hrs in this case), orbital shaking results in greater monomer loss relative to the EFD (which is performed in these experiments over 20 mins). Notwithstanding the differences in magnitude, the patterns of protection are similar for all of the platform formulations between the EFD and the shaking study: Fc-XEng is resistant to aggregation compared to wild-type (85 % and 96 % loss of monomer, respectively), and PS80 is protective in both HS and HSA buffers. In contrast to these similarities, it is interesting to note that the deleterious effect of arginine on solubility is not observed after orbital shaking, again pointing at different aggregation mechanisms between these two methods. Together, the data highlight that hydrodynamic stress studies can identify platform buffers that protect against EFD-induced aggregation. The degree of protection is dependent on the molecule under investigation, in addition to the mechanism of aggregation under different flow regimes.

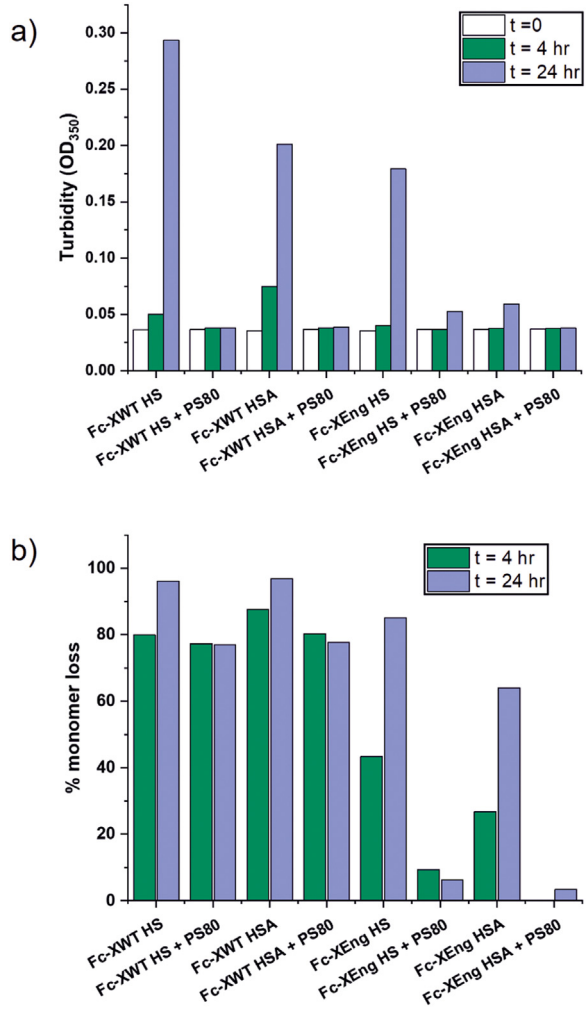

Figure 7. Orbital shaking analysis of Fc-fusion proteins in different platform formulations. a) Quantification of turbidity at 350 nm (OD_{350}) for Fc-XWT and Fc-XEng in the four main platform formulations. b) Quantification of percentage monomer remaining in solution by HPLC for the Fc-XWT and Fc-XEng proteins above. Shaking was carried out for 0, 4 or 24 h (0 h = incubated for a day at room temperature with no shaking). HS = histidine-sucrose, HSA = histidine-sucrose-arginine, PS80 = 0.02 % (w/v) polysorbate 80. *N* = 1 all samples.

Discussion

Decades of research and development in protein and formulation science[19] have allowed many mAb formulations to share common buffer and excipient combinations which maintain the physicochemical stability of the mAb and allow successful delivery into patients. These 'platform formulations' help accelerate the development of these molecules as therapies.[23] As the amino acid sequence, structure and dynamics of a mAb[18,30,63,64] may lead to aberrant biophysical behaviour, a 'one-size-fits-all' approach to formulation may not necessarily work for all molecules. This is a particular challenge for newer modalities, such as fusion proteins, as the number of approved products (<20, to date)[10] and body of literature surrounding their developability, is much smaller relative to their full-length monoclonal antibody counterparts.[24] Additionally, Fc-fusion proteins have a wide array of sequences, topologies and formats,[8,10] making the design of a single platform formulation challenging.

The main drivers of this research were to better understand the utility of the EFD in establishing the fitness of platform formulations early in development, as well as identifying molecules which suit these platform formulations. For example, our previous work showed that high concentrations of arginine (125 mM, 5x higher than the amount used in this work) can reduce the aggregation of a sensitive IgG1 under flow.[50] Comparing the EFD-induced aggregation of the mAbP1–8 panel with their AS and real-time stability data showed that mAbP1 was the least aggregation-prone molecule. This was achieved using small amounts of material (generating each landscape consumed ~11 mg of material in total) and a few days' work per molecule. We note, however, that the majority of mAbs displayed similar levels of EFD-induced aggregation, suggesting that EFD screening may be more appropriate earlier in candidate selection. If a rapid result was required, we have shown that 200 passes at 5 mg/mL (using 0.5 mL) 8 mm/s (which takes 20 min to complete), provides adequate discrimination between different formulations (Fig. 5) and is much faster than the orbital shaking method, using half the sample volume.

Despite the simplicity of the EFD design which has well-defined hydrodynamic flow fields (extensional flow and shear flow) and known glass-liquid interface surface area,[49,50] it is clear that many parameters can affect the extent of EFD-induced aggregation. For example, when the plunger velocity increases, the exposure time of a protein to extensional flow decreases whilst there is a concomitant increase in the magnitude of the force (strain rate) applied.[49] In the work presented for HS buffer, higher velocities led to the formation of aggregates of broader dispersity, with such aggregates better able to scatter light (Fig. 2). The aggregation landscapes suggest that the amount of monomer lost was similar across the different plunger velocities. As the timescales differ widely between each experiment, it could be that longer timescales (at 4 mm/s) allow for the coalescence of aggregates into larger species,[65] which may be broken up when the EFD experiments are carried out at higher plunger velocities.[66] These results could have implications in bioprocessing steps where extensional flows are found, namely the removal of proteinaceous aggregates by membrane filters.[35,67] Furthermore the shear rates in the capillary of the EFD have a similar magnitude to those found in fill-finish operations, as reviewed by Bee et al.[68]

It was also clear from increasing the protein concentration from 0.5 to 50 mg/mL that there is an inverse-concentration dependence on EFD-induced aggregation for the mAbP3–6 molecules in HS buffer. There is an established literature precedence towards surface-mediated protein aggregation explaining inverse concentration-dependent protein aggregation phenomena.[31,44,57,69–71] The change in relative and absolute extents of aggregation as a function of initial protein concentration (Fig. S7a) clearly shows that a switch in mechanism occurs between 0.5–5 mg/mL. While some groups have suggested that bulk flows can perturb protein structure[72–74] and induce protein aggregation,[34,49,75] this is still controversial.[70,71] For this mechanism, bulk flow may induce conformational changes in proteins,[73,74,76] exposing previously solvent sequestered residues (which can be chemically modified only in presence of flow)[49,77] triggering the formation of aggregation-prone species.[49,75–77] Alternatively, hydrodynamic flow may simply act to accelerate the turnover of aggregation-prone protein conformations adsorbed onto air-water or solid-water interfaces into bulk solution.[31,41–44,46–48,55,70,71,78–80] For example in orbital shaking experiments, the size of the air-water interfaces formed and frequency of their turnover, can influence the extent of aggregation observed.[78,81] For solid-liquid interfaces, the chemistry of the solvent-facing substrate in addition to its surface area has been previously shown to affect protein aggregation propensity, using similar devices.[31,62] Work is ongoing to investigate the kinetic mechanism of EFD-induced aggregation showing that the presence of both extensional flow and solid-liquid interfaces are pivotal to the mechanism, with cavitation not occurring under the conditions tested (manuscript in preparation). To explore the synergy between interfaces and extensional flow in greater detail and to assess its importance to biopharmaceutical manufacture, development of a suite of devices composed of materials commonly found in processing is ongoing.

The addition of surfactant into the platform buffers only suppressed the aggregation of mAbP6, but was universally protective for both fusion proteins in both HS and HSA buffer. This differential protection may reflect distinct aggregation mechanisms for mAbs and fusion proteins. For example, the propensity for the Fc-fusions to aggregate *via* an interfacial-dominant mechanism is clear from the literature,[46,62] as observed during the use of a stainless steel HPLC system in this study. This may mean single-use bioprocessing equipment is better suited to fusion proteins, rather than traditional stainless-steel setups.

By contrast to the clearly protective role of PS80, arginine did not reduce EFD-induced aggregation and a significant protective effect was only observed for the fusion protein Fc-XEng when stressed using the orbital shaker. This contrasts with three IgG1's which showed reduced aggregation propensity in the EFD when stressed in the presence of this additive.[50] Strikingly, a comparison of EFD-induced aggregation in HS and HSA buffers in the presence of PS80 suggests that arginine may even suppress the protection afforded by surfactant. Whether this effect is due to direct interaction between these excipients, the complex amphipathic nature of the arginine leading to a variety of possible interaction modes with proteins (e.g. blocking exposed hydrophobic or charged patches on proteins),[82] the influence of counterions in the formulation affecting arginine's protective interaction modes,[60] or the ability of arginine to thermodynamically destabilize some proteins,[59] is unclear. It should be noted that arginine was not included in any of the original formulations used for the AS and real-time stability study.

The EFD features solid-liquid interfaces, with air-water interfaces removed prior to stress. The addition of surfactant to the HS and HSA buffers reduced aggregation after 200 passes for both fusion proteins. In the orbital shaking study, the main perturbants present are air-water interface turnover and shear flow.[36,48,83,84] Surfactants are included in therapeutic protein formulations to protect against interfacial aggregation.[22,34,85,86] PS80 has a larger protective effect in orbital shaking, with only a 5 % loss of monomer for the Fc-XEng protein after 24 hrs in HSA + PS80 vs 40 % loss in the EFD.

In conclusion, our studies show platform formulations can modulate the aggregation of antibody-based proteins under flow and that the size distribution of the aggregates which subsequently form is sensitive to the flow used in the EFD. Where interfacial aggregation dominates such as the air-water interfaces formed during orbital shaking, the presence of surfactant in the form of polysorbate 80 can confer significant protection against aggregation of fusion proteins. These results highlight the necessity of platform formulation screening to minimise aggregation, with surfactants being the most crucial component to protect against the effects of flow. While both the EFD and orbital shaking quantify the effects of mechanical agitation (which comprises both hydrodynamic flow and interfacial stresses) the methods appear to differ with respect to the underlying mechanism driving aggregation. The work presented will inform further studies to better understand this process, which is clearly modulated by the formulation environment.

Declaration of data availability

For the purpose of open access, the authors have applied a Creative Commons Attribution (CC BY) licence to any Author Accepted Manuscript version arising from this submission. The datasets used and/or analyzed during the current study are available from the corresponding authors on reasonable request.

Funding

L.F.W was funded for this work by an EPSRC Doctoral Prize Fellowship (EP/IO3327/1) and by Pfizer LLC. SER holds a Royal Society Research Professorship (RSRP\R1\211057). The Shimadzu HPLC was funded by the Wellcome Trust (WT204963). We thank the School of Chemistry (University of Leeds) for HPLC access during the study.

Supplementary Information

Details of Dynamic Light Scattering (DLS) measurements, real-time (5 °C) and accelerated (25 °C) stability and orbital shaking are provided in the Supplementary Methods. We also include supporting data and tables, as referenced in the text.

Declaration of Competing Interest

The authors declare that they have no known competing financial interests or personal relationships that could have appeared to influence the work reported in this paper.

CRediT authorship contribution statement

Leon F. Willis: Conceptualization, Methodology, Investigation, Formal analysis, Visualization, Writing – original draft, Writing – review & editing. **Vishal Toprani:** Conceptualization, Methodology, Investigation, Formal analysis, Supervision, Project administration, Writing – review & editing. **Sashini Wijetunge:** Investigation, Formal analysis. **Annette Sievers:** Methodology, Supervision. **Laura Lin:** Methodology, Supervision. **Jeanine Williams:** Investigation. **Tom J. Crowley:** Methodology, Supervision, Funding acquisition. **Sheena E. Radford:** Supervision, Writing – review & editing. **Nikil Kapur:** Methodology, Supervision, Writing – review & editing. **David J. Brockwell:** Conceptualization, Methodology, Supervision, Funding acquisition, Writing – original draft, Writing – review & editing.

Acknowledgments

We acknowledge Dr Iain Manfield (University of Leeds) for assistance with HPLC at the start of the project, the School of Chemistry (University of Leeds) for use of HPLC, Mr G. Nasir Khan for his excellent technical assistance throughout the project, Mr Nathan Berry (Nexus, University of Leeds) for administrative assistance throughout the project and members of the Radford and Brockwell laboratories for useful discussions.

Supplementary materials

Supplementary material associated with this article can be found in the online version at doi:10.1016/j.xphs.2023.10.031.

References

1. Tiller K.E., Tessier P.M. Advances in antibody design. *Annu Rev Biomed Eng*. 2015;17:191–216. doi:10.1146/annurev-bioeng-071114-040733.
2. Rabia L.A., Zhang Y., Ludwig S.D., Julian M.C., Tessier P.M. Net charge of antibody complementarity-determining regions is a key predictor of specificity. *Protein Eng. Design Selection*. 2019:1–10. doi:10.1093/protein/gzz002.
3. Mullard A. FDA approves 100th monoclonal antibody product. *Nat Rev Drug Discov*. 2021;20(7):491–495. https://doi.org/10.1038/d41573-021-00079-7.
4. Kaplon H, Chenoweth A, Crescioli S, Reichert JM. Antibodies to watch in 2022. *MAbs*. 2022;14(1). https://doi.org/10.1080/19420862.2021.2014296.
5. Goulet DR, Atkins WM. Considerations for the design of antibody-based therapeutics. *J Pharm Sci*. 2020;109(1):74–103. https://doi.org/10.1016/j.xphs.2019.05.031.
6. Wu L, Seung E, Xu L, et al. Trispecific antibodies enhance the therapeutic efficacy of tumor-directed T cells through T cell receptor co-stimulation. *Nat Cancer*. 2020;1(1):86–98. https://doi.org/10.1038/s43018-019-0004-z.
7. Kontermann RE, Brinkmann U. Bispecific antibodies. *Drug Discov Today*. 2015;20(7):838–847. https://doi.org/10.1016/j.drudis.2015.02.008.
8. Wilkinson I, Hale G. Systematic analysis of the varied designs of 819 therapeutic antibodies and Fc fusion proteins assigned international nonproprietary names. *MAbs*. 2022;14(1): 2123299. https://doi.org/10.1080/19420862.2022.2123299.
9. Strohl WR. Current progress in innovative engineered antibodies. *Protein Cell*. 2018;9(1):86–120. https://doi.org/10.1007/s13238-017-0457-8.

10. Duivelshof BL, Murisier A, Camperi J, et al. Therapeutic Fc-fusion proteins: current analytical strategies. *J Sep Sci*. 2021;44(1):35–62. https://doi.org/10.1002/jssc.202000765.
11. Wang W, Roberts CJ. Protein aggregation – Mechanisms, detection, and control. *Int J Pharm*. 2018;550(1–2):251–268. https://doi.org/10.1016/j.ijpharm.2018.08.043.
12. Cromwell MEM, Hilario E, Jacobson F. Protein aggregation and bioprocessing. *AAPS J*. 2006;8(3):E572–E579. https://doi.org/10.1208/aapsj080366.
13. Roberts CJ. Protein aggregation and its impact on product quality. *Curr Opin Biotechnol*. 2014;30C:211–217. https://doi.org/10.1016/j.copbio.2014.08.001.
14. Das TK, Chou DK, Jiskoot W, Arosio P. Nucleation in protein aggregation in biotherapeutic development: a look into the heart of the event. *J Pharm Sci*. 2022;111(4):951–959. https://doi.org/10.1016/j.xphs.2022.01.017.
15. Eyes TJ, Austerberry JI, Dearman RJ, et al. Identification of B cell epitopes enhanced by protein unfolding and aggregation. *Mol Immunol*. 2019;105:181–189. https://doi.org/10.1016/j.molimm.2018.11.020.
16. Rosenberg AS. Effects of protein aggregates: an immunologic perspective. *AAPS J*. 2006;8(3):E501–E507. https://doi.org/10.1208/aapsj080359.
17. Carter PJ, Rajpal A. Designing antibodies as therapeutics. *Cell*. 2022;185(15):2789–2805. https://doi.org/10.1016/j.cell.2022.05.029.
18. Dobson CL, Devine PWA, Phillips JJ, et al. Engineering the surface properties of a human monoclonal antibody prevents self-association and rapid clearance in vivo. *Sci Rep*. 2016;6:38644. https://doi.org/10.1038/srep38644.
19. Wang W, Ohtake S. Science and art of protein formulation development. *Int J Pharm*. 2019;568(July): 118505. https://doi.org/10.1016/j.ijpharm.2019.118505.
20. Kelley B. Industrialization of mAb production technology: the bioprocessing industry at a crossroads. *MAbs*. 2009;1(5):443–452. https://doi.org/10.4161/mabs.1.5.9448.
21. Wang W. Advanced protein formulations. *Protein Sci*. 2015;24(7):1031–1039. https://doi.org/10.1002/pro.2684.
22. Strickley RG, Lambert WJ. A review of formulations of commercially available antibodies. *J Pharm Sci*. 2021;110(7). https://doi.org/10.1016/j.xphs.2021.03.017. 2590-2608.e56.
23. Goldberg DS, Lewus RA, Esfandiary R, et al. Utility of high throughput screening techniques to predict stability of monoclonal antibody formulations during early stage development. *J Pharm Sci*. 2017;106(8):1971–1977. https://doi.org/10.1016/j.xphs.2017.04.039.
24. Svilenov HL, Arosio P, Menzen T, Tessier P, Sormanni P. Approaches to expand the conventional toolbox for discovery and selection of antibodies with drug-like physicochemical properties. *MAbs*. 2023;15(1): 2164459. https://doi.org/10.1080/19420862.2022.2164459.
25. Bailly M, Mieczkowski C, Juan V, et al. Predicting antibody developability profiles through early stage discovery screening. *MAbs*. 2020;12(1). https://doi.org/10.1080/19420862.2020.1743053.
26. Svilenov HL, Winter G. Formulations that suppress aggregation during long-term storage of a bispecific antibody are characterized by high refoldability and colloidal stability. *J Pharm Sci*. 2020;109(6):2048–2058. https://doi.org/10.1016/j.xphs.2020.03.011.
27. Kopp MRG, Wolf Pérez AM, Zucca MV, et al. An accelerated surface-mediated stress assay of antibody instability for developability studies. *MAbs*. 2020;12(1): 1815995. https://doi.org/10.1080/19420862.2020.1815995.
28. Xu Y, Wang D, Mason B, et al. Structure, heterogeneity and developability assessment of therapeutic antibodies. *MAbs*. 2019;11(2):239–264. https://doi.org/10.1080/19420862.2018.1553476.
29. Menzen T, Friess W. Temperature-ramped studies on the aggregation, unfolding, and interaction of a therapeutic monoclonal antibody. *J Pharm Sci*. 2014;103(2):445–455. https://doi.org/10.1002/jps.23827.
30. Codina N, Hilton D, Zhang C, et al. An expanded conformation of an antibody Fab region by X-Ray scattering, molecular dynamics, and smFRET identifies an aggregation mechanism. *J Mol Biol*. 2019;431(7):1409–1425. https://doi.org/10.1016/j.jmb.2019.02.009.
31. Grigolato F, Arosio P. Synergistic effects of flow and interfaces on antibody aggregation. *Biotechnol Bioeng*. 2020;117(2):417–428. https://doi.org/10.1002/bit.27212.
32. Sreenivasan S, Jiskoot W, Rathore AS. Rapid aggregation of therapeutic monoclonal antibodies by bubbling induced air/liquid interfacial and agitation stress at different conditions. *Eur J Pharm Biopharm*. 2021;168:97–109. https://doi.org/10.1016/j.ejpb.2021.08.010.
33. Nowak CK, Cheung JM, Dellatore S, et al. Forced degradation of recombinant monoclonal antibodies: a practical guide. *MAbs*. 2017;9(8):1217–1230. https://doi.org/10.1080/19420862.2017.1368602.
34. Grabarek AD, Bozic U, Rousel J, et al. What makes Polysorbate functional? Impact of polysorbate 80 grade and quality on IgG stability during mechanical stress. *J Pharm Sci*. 2020;109(1):871–880. https://doi.org/10.1016/j.xphs.2019.10.015.
35. Schwaller C, Fokkens K, Helmreich B, Drewes JE. CFD simulations of flow fields during ultrafiltration: effects of hydrodynamic strain rates with and without a particle cake layer on the permeation of mobile genetic elements. *Chem Eng Sci*. 2022;254:117606. https://doi.org/10.1016/j.ces.2022.117606.
36. Koepf E, Eisele S, Schroeder R, Brezesinski G, Friess W. Notorious but not understood: how liquid-air interfacial stress triggers protein aggregation. *Int J Pharm*. 2018;537(1–2):202–212. https://doi.org/10.1016/j.ijpharm.2017.12.043.
37. Zhang Y, Han D, Dou Z, et al. The interface motion and hydrodynamic shear of the liquid slosh in syringes. *Pharm Res*. 2021;38(2):257–275. https://doi.org/10.1007/s11095-021-02992-3.
38. Eshraghi J, Veilleux JC, Shi G, Collins D, Ardekani AM, Vlachos PP. Assessment of cavitation intensity in accelerating syringes of spring-driven autoinjectors. *Pharm Res*. 2022;39(9):2247–2261. https://doi.org/10.1007/s11095-022-03334-7.
39. Blümel M, Liu J, de Jong I, et al. Current industry best practice on in-use stability and compatibility studies for biological products. *J Pharm Sci*. 2023. https://doi.org/10.1016/j.xphs.2023.05.002.
40. Fleischman ML, Chung J, Paul EP, Lewus RA. Shipping-induced aggregation in therapeutic antibodies: utilization of a scale-down model to assess degradation in monoclonal antibodies. *J Pharm Sci*. 2017;106(4):994–1000. https://doi.org/10.1016/j.xphs.2016.11.021.
41. Wu H, Randolph TW. Aggregation and particle formation During pumping of an antibody formulation are controlled by electrostatic interactions between pump surfaces and protein molecules. *J Pharm Sci*. 2020. https://doi.org/10.1016/j.xphs.2020.01.023.
42. Wu H, Chisholm CF, Puryear M, et al. Container surfaces control initiation of cavitation and resulting particle formation in protein formulations after application of mechanical shock. *J Pharm Sci*. 2020;109(3):1270–1280. https://doi.org/10.1016/j.xphs.2019.11.015.
43. Kalonia CK, Heinrich F, Curtis JE, Raman S, Miller MA, Hudson SD. Protein adsorption and layer formation at the stainless steel-solution interface mediates shear-induced particle formation for an IgG1 monoclonal antibody. *Mol Pharm*. 2018;15(3):1319–1331. https://doi.org/10.1021/acs.molpharmaceut.7b01127.
44. Thite NG, Ghazvini S, Wallace N, Feldman N, Calderon CP, Randolph TW. Interfacial adsorption controls particle formation in antibody formulations subjected to extensional flows and hydrodynamic shear. *J Pharm Sci*. 2023. https://doi.org/10.1016/j.xphs.2023.07.010.
45. Kopp MRG, Capasso Palmiero U, Arosio P. A Nanoparticle-based assay to evaluate surface-induced antibody instability. *Mol Pharm*. 2020;17(3):909–918. https://doi.org/10.1021/acs.molpharmaceut.9b01168.
46. Johann F, Wöll S, Winzer M, Snell J, Valldorf B, Gieseler H. Miniaturized forced degradation of therapeutic proteins and ADCs by agitation-induced aggregation using orbital shaking of microplates. *J Pharm Sci*. 2022;111(5):1401–1413. https://doi.org/10.1016/j.xphs.2021.09.027.
47. Wiesbauer J, Cardinale M, Nidetzky B. Shaking and stirring: comparison of controlled laboratory stress conditions applied to the human growth hormone. *Process Biochem*. 2013;48(1):33–40. https://doi.org/10.1016/j.procbio.2012.11.007.
48. Kiese S, Papppenberger A, Friess W, Mahler HC. Shaken, not stirred: mechanical stress testing of an IgG1 antibody. *J Pharm Sci*. 2008;97(10):4347–4366. https://doi.org/10.1002/jps.21328.
49. Dobson J, Kumar A, Willis LF, et al. Inducing protein aggregation by extensional flow. *Proc Natl Acad Sci*. 2017;114(18):4673–4678. https://doi.org/10.1073/pnas.1702724114.
50. Willis LF, Kumar A, Dobson J, et al. Using extensional flow to reveal diverse aggregation landscapes for three IgG1 molecules. *Biotechnol Bioeng*. 2018;115(5):1216–1225. https://doi.org/10.1002/bit.26543.
51. Willis LF, Kumar A, Jain T, et al. The uniqueness of flow in probing the aggregation behavior of clinically relevant antibodies. *Eng Rep*. 2020;2(5). https://doi.org/10.1002/eng2.12147.
52. Jain T, Sun T, Durand S, et al. Biophysical properties of the clinical-stage antibody landscape. *Proc Natl Acad Sci*. 2017;114(5):944–949. https://doi.org/10.1073/pnas.1616408114.
53. Minton AP. Recent applications of light scattering measurement in the biological and biopharmaceutical sciences. *Anal Biochem*. 2016;501:4–22. https://doi.org/10.1016/j.ab.2016.02.007.
54. Wälchli R, Vermeire PJ, Massant J, Arosio P. Accelerated aggregation studies of monoclonal antibodies: considerations for storage stability. *J Pharm Sci*. 2020;109(1):595–602. https://doi.org/10.1016/j.xphs.2019.10.048.
55. Li J, Krause ME, Chen X, et al. Interfacial stress in the development of biologics: fundamental understanding, current practice, and future perspective. *AAPS J*. 2019;21(3). https://doi.org/10.1208/s12248-019-0312-3.
56. Halley J, Chou YR, Cicchino C, et al. An industry perspective on forced degradation studies of biopharmaceuticals: survey outcome and recommendations. *J Pharm Sci*. 2020;109(1):6–21. https://doi.org/10.1016/j.xphs.2019.09.018.
57. Treuheit MJ, Kosky AA, Brems DN. Inverse relationship of protein concentration and aggregation. *Pharm Res*. 2002;19(4):511–516. https://doi.org/10.1023/A:1015108115452.
58. Hofmann M, Gieseler H. Predictive screening tools used in high-concentration protein formulation development. *J Pharm Sci*. 2018;107(3):772–777. https://doi.org/10.1016/j.xphs.2017.10.036.
59. Kim NA, Hada S, Thapa R, Jeong SH. Arginine as a protein stabilizer and destabilizer in liquid formulations. *Int J Pharm*. 2016;513(1–2):26–37. https://doi.org/10.1016/j.ijpharm.2016.09.003.
60. Zhang J, Frey V, Corcoran M, Zhang-Van Enk J, Subramony JA. Influence of arginine salts on the thermal stability and aggregation kinetics of monoclonal antibody: dominant role of anions. *Mol Pharm*. 2016;13(10):3362–3369. https://doi.org/10.1021/acs.molpharmaceut.6b00255.
61. Blas P, Tolner B, Ward J, Chester K, Hoare M. The use of a surface active agent in the protection of a fusion protein during bioprocessing. *Biotechnol Bioeng*. 2018;115(11):2760–2770. https://doi.org/10.1002/bit.26817.
62. Defante AP, Kalonia CK, Keegan E, et al. The impact of the metal interface on the stability and quality of a therapeutic fusion protein. *Mol Pharm*. 2020;17(2):569–578. https://doi.org/10.1021/acs.molpharmaceut.9b01000.
63. Raybould MIJ, Marks C, Krawczyk K, et al. Five computational developability guidelines for therapeutic antibody profiling. *Proc Natl Acad Sci*. 2019;116(10):4025–4030. https://doi.org/10.1073/pnas.1810576116.

64. Cornwell O, Bond NJ, Radford SE, Ashcroft AE. Long-range conformational changes in monoclonal antibodies revealed using FPOP-LC-MS/MS. *Anal Chem*. 2019;91 (23):15163–15170. https://doi.org/10.1021/acs.analchem.9b03958.
65. Nicoud L, Owczarz M, Arosio P, Morbidelli M. A multiscale view of therapeutic protein aggregation: a colloid science perspective. *Biotechnol J*. 2015;10(3):367–378. https://doi.org/10.1002/biot.201400858.
66. Ren Z, Harshe YM, Lattuada M. Influence of the potential well on the breakage rate of colloidal aggregates in simple shear and uniaxial extensional flows. *Langmuir*. 2015;31(21):5712–5721. https://doi.org/10.1021/la504966y.
67. Baek Y, Zydney AL. Intermolecular interactions in highly concentrated formulations of recombinant therapeutic proteins. *Curr Opin Biotechnol*. 2018;53:59–64. https://doi.org/10.1016/j.copbio.2017.12.016.
68. Bee JS, Stevenson JL, Mehta B, et al. Response of a concentrated monoclonal antibody formulation to high shear. *Biotechnol Bioeng*. 2009;103(5):936–943. https://doi.org/10.1002/bit.22336.
69. Bee JS, Chiu D, Sawicki S, et al. Monoclonal antibody interactions with micro- and nanoparticles: adsorption, aggregation, and accelerated stress studies. *J Pharm Sci*. 2009;98(9):3218–3238. https://doi.org/10.1002/jps.21768.
70. Grigolato F, Arosio P. The role of surfaces on amyloid formation. *Biophys Chem*. 2021;270: 106533. https://doi.org/10.1016/j.bpc.2020.106533.
71. Kopp MRG, Grigolato F, Zürcher D, et al. Surface-induced protein aggregation and particle formation in biologics: current understanding of mechanisms, detection and mitigation strategies. *J Pharm Sci*. 2023;112(2):377–385. https://doi.org/10.1016/j.xphs.2022.10.009.
72. Papeż P, Merzel F, Praprotnik M. Rotational dynamics of a protein under shear flow studied by the Eckart frame formalism. *J Phys Chem B*. 2023;127(33):7231–7243. https://doi.org/10.1021/acs.jpcb.3c02324.
73. Ashton L, Dusting J, Imomoh E, Balabani S, Blanch EW. Susceptibility of different proteins to flow-induced conformational changes monitored with Raman spectroscopy. *Biophys J*. 2010;98(4):707–714. https://doi.org/10.1016/j.bpj.2009.10.010.
74. Bekard IB, Asimakis P, Teoh CL, et al. Bovine serum albumin unfolds in Couette flow. *Soft Matter*. 2012;8:385. https://doi.org/10.1039/c1sm06704d.
75. Simon S, Krause HJ, Weber C, Peukert W. Physical degradation of proteins in well-defined fluid flows studied within a four-roll apparatus. *Biotechnol Bioeng*. 2011;108(12):2914–2922. https://doi.org/10.1002/bit.23257.
76. Bekard IB, Asimakis P, Bertolini J, Dunstan DE. The effects of shear flow on protein structure and function. *Biopolymers*. 2011;95(11):733–745. https://doi.org/10.1002/bip.21646.
77. Hakala TA, Yates EV, Challa PK, et al. Accelerating reaction rates of biomolecules by using shear stress in artificial capillary systems. *J Am Chem Soc*. 2021;143 (40):16401–16410. https://doi.org/10.1021/jacs.1c03681.
78. Dasnoy S, Illartin M, Queffelec J, Nkunku A, Peerboom C. Combined effect of shaking orbit and vial orientation on the agitation-induced aggregation of proteins. *J Pharm Sci*. 2023. https://doi.org/10.1016/j.xphs.2023.08.016.
79. Bai G, Bee JS, Biddlecombe JG, Chen Q, Leach WT. Computational fluid dynamics (CFD) insights into agitation stress methods in biopharmaceutical development. *Int J Pharm*. 2012;423(2):264–280. https://doi.org/10.1016/j.ijpharm.2011.11.044.
80. Fanthom TB, Wilson C, Gruber D, Bracewell DG. Solid-solid interfacial contact of tubing walls drives therapeutic protein aggregation during peristaltic pumping. *J Pharm Sci*. 2023. https://doi.org/10.1016/j.xphs.2023.08.012.
81. Kizuki S, Wang Z, Torisu T, Yamauchi S, Uchiyama S. Relationship between aggregation of therapeutic proteins and agitation parameters: acceleration and frequency. *J Pharm Sci*. 2022;000:1–14. https://doi.org/10.1016/j.xphs.2022.09.022.
82. Shukla D, Trout BL. Interaction of arginine with proteins and the mechanism by which it inhibits aggregation. *J Phys Chem B*. 2010;114(42):13426–13438. https://doi.org/10.1021/jp108399g.
83. Daniels AL, Calderon CP, Randolph TW. Machine learning and statistical analyses for extracting and characterizing “fingerprints” of antibody aggregation at container interfaces from flow microscopy images. *Biotechnol Bioeng*. 2020;117 (11):3322–3335. https://doi.org/10.1002/bit.27501.
84. Zhou J, Ruggeri FS, Zimmermann MR, et al. Effects of sedimentation, microgravity hydrodynamic mixing and air-water interface on α-synuclein amyloid formation. *Chem Sci*. 2020. https://doi.org/10.1039/d0sc00281j.
85. Kerwin BA. Polysorbates 20 and 80 used in the formulation of protein biotherapeutics: structure and degradation pathways. *J Pharm Sci*. 2008;97(8):2924–2935. https://doi.org/10.1002/JPS.21190.
86. Zoeller MP, Hafiz S, Marx A, Erwin N, Fricker G, Carpenter JF. Exploring the protein stabilizing capability of surfactants against agitation stress and the underlying mechanisms. *J Pharm Sci*. 2022. https://doi.org/10.1016/j.xphs.2022.09.004.
87. Weinbuch D, Cheung JK, Ketelaars J, et al. Nanoparticulate impurities in pharmaceutical-grade sugars and their interference with light scattering-based analysis of protein formulations. *Pharm. Res.*. 2015;32:2419–2427. https://doi.org/10.1007/s11095-015-1634-1.